American Mineralogist, Volume 71, pages 38–50, 1986

Raman spectroscopic study of the SiO_2–Al_2O_3–K_2O vitreous system: distribution of silicon second neighbors

FLORENT DOMINE

CNRS, ER 224, Laboratoire de Geologie
Ecole Normale Superieure, 46 rue d'Ulm
75230 Paris Cedex 05, France

AND BERNARD PIRIOU

Laboratoire des elements de transition dans les solides
CNRS, 92120 Meudon-Bellevue, France

Abstract

Raman VV and VH spectra of seven glass compositions in the system SiO_2–Al_2O_3–K_2O are presented. Interest is focused on the high frequency envelope of the spectra (850–1250 cm^{-1}) and the model proposed to decompose this envelope into its component bands suggests that Raman response is characteristic of small entities, here silicon, and its first and second neighbors. Assuming a random distribution of silicon second neighbors, seven environments are found in a large enough proportion to show some detectable Raman signal. The decomposition is made with one or several bands for each of these seven environments, whose frequencies and widths do not vary with composition.

Quantitative comparison of VV and VH spectra demonstrate the overall consistency of the band fittings. Quantitative comparison of data expected from a random distribution with experimental data show that aluminium favors fully polymerized environments (without non-bridging oxygens) and that in the presence of aluminium, network modifying potassium ions tend to concentrate in less polymerized environments. This can be explained by the low charge density of potassium and a repulsion between Al and K as silicon second neighbors.

A non-random statistical distribution of silicon second neighbors is then calculated with 6 parameters representing interactions between cations. Interest is focused on parameters x and y defined as $p(Al\backslash K) = xp(Al)$, $p(K\backslash K) = yp(K)$, where $p(Al\backslash K)$ and $p(K\backslash K)$ are the probabilities of having Al or K, respectively, as a silicon second neighbor if K is also a second neighbor and p(Al) and p(K) are the probabilities defined in the random distribution. By minimizing the difference between experimental and calculated data, we find $x = 0.55$ and $y = 4.65$, thus quantifying the experimentally observed Al–K and K–K interaction in the composition range studied.

Introduction

The knowledge of the structure of silicate melts is essential to the understanding of magmatic processes. Raman spectroscopy has been a method commonly used to investigate the structure of vitreous silicates. The Raman studies have been carried out on quenched melts (glasses) since it has been established that the vibrational spectra of non-crystalline silicates do not vary significantly with temperature (Sweet and White, 1969; Seifert et al., 1981a; Domine and Piriou, 1983).

Most Raman studies of silicate glasses have considered binary SiO_2–M_2O (M = Li, Na, K, $Ca_{0.5}$) systems without aluminium (see, for example, Brawer and White, 1975; Konijnendijk and Stevels, 1976; Virgo et al., 1980; Mysen et al., 1982a); however several binary aluminium bearing systems have also been investigated. These include the SiO_2–$MAlO_2$ systems (M = Na, K, $Ca_{0.5}$, $Mg_{0.5}$) (McMillan et al., 1982; Seifert et al., 1982). These studies of simple binary systems are important, however melts of geological interest are much more complex systems which include structural features such as silicon and aluminium as network formers and non-bridging oxygens due to various network modifiers. None of the work mentioned above involves glasses with both network forming aluminium and NBO. By BO we mean an oxygen that is bonded to two network formers. By NBO, we mean an oxygen that is bonded to only one network former. NBO's therefore have a negative charge which is balanced by a nearby network modifier, so NBO's can be said to be also bonded to network modifiers. Some work has been done on those

0003–004X/86/0102–0038$02.00

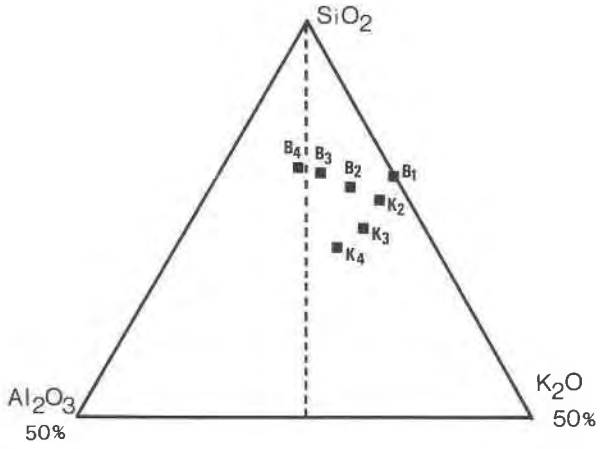

Fig. 1. Composition of the samples studied by Raman spectroscopy.

more complex systems (Konijnendijk, 1975; Mysen et al., 1980, 1981) but since very few compositions were investigated only limited results were obtained.

The purpose of the present work is to acquire information concerning the structure of the silica rich part of the SiO_2–Al_2O_3–K_2O system, where both aluminium and NBO's coexist.

Experimental techniques

The samples were melted from gels prepared according to the method described by Roy (1956). The experimental compositions were synthesized from high purity orthotetraethylsilicate, aluminium nitrate and potassium carbonate. The gels were progressively heated to 1200–1600°C for 2–24 hours depending on their compositions, then reground and reheated to ensure chemical homogeneity. Since the crystallization rate of these compositions is very low, quenching was done by simply removing the sample from the furnace.

The chemical composition of the samples were determined with a CAMEBAX electron microprobe, using conditions suitable for glass analysis (1.5 nA, 15 kV, beam diameter 12 μm, counting time 30 s). The microprobe analysis, given in Figure 1 and Table 1, demonstrate homogeneous glass compositions. The B series has a constant silica content, with variable K/Al ratio, whereas the K series has a constant K/Al ratio with variable silica content. B4 is peraluminous, the others all being peralkaline. 5 mm to 1 cm samples were then cut and polished for 90° Raman scattering. All samples were physically homogeneous and bubble free, except B4 and K4. The presence of bubbles in these 2 samples can account for the lesser quality found in their spectra (Figs. 2 and 3). The glasses were excited with the 4579 Å line of a spectra

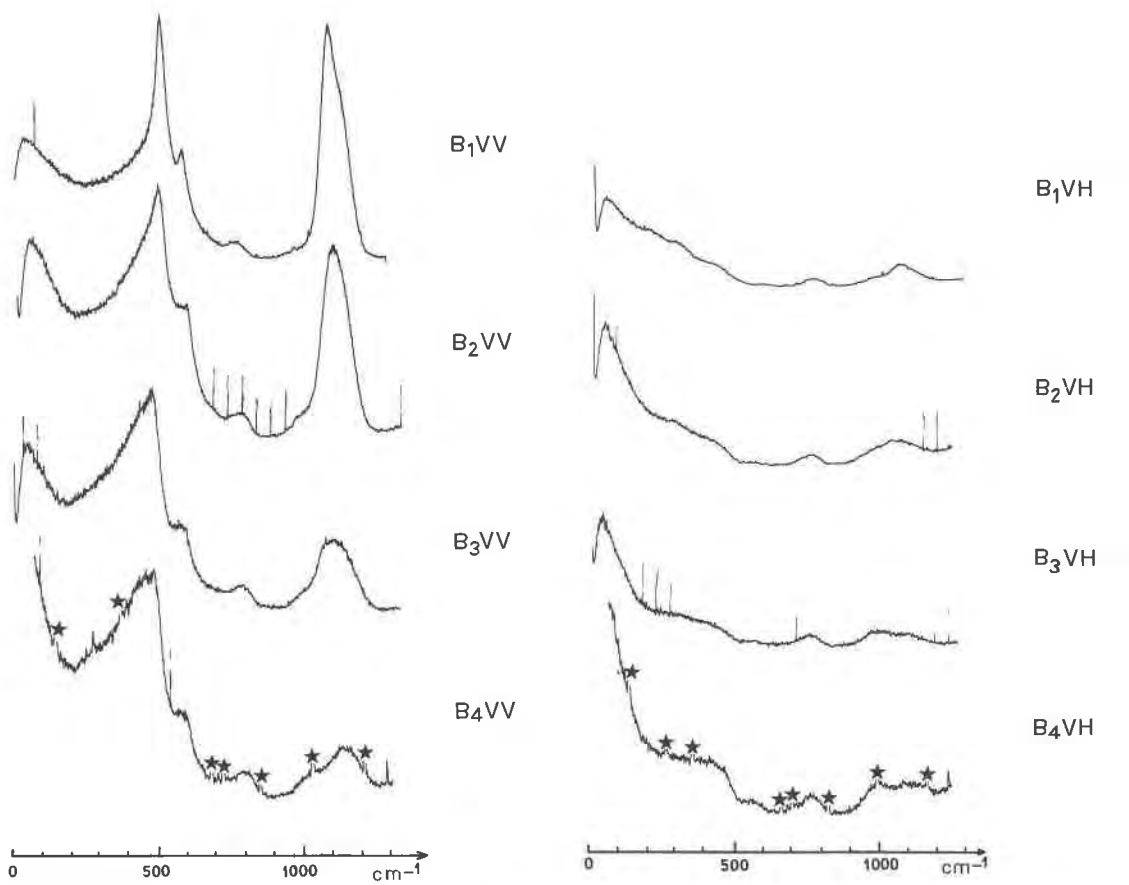

Fig. 2. Raman diffusion spectra of B series samples. VV: parallel polarization, VH: perpendicular polarization, stars indicate laser plasma lines which are diffused by small bubbles contained in the glass.

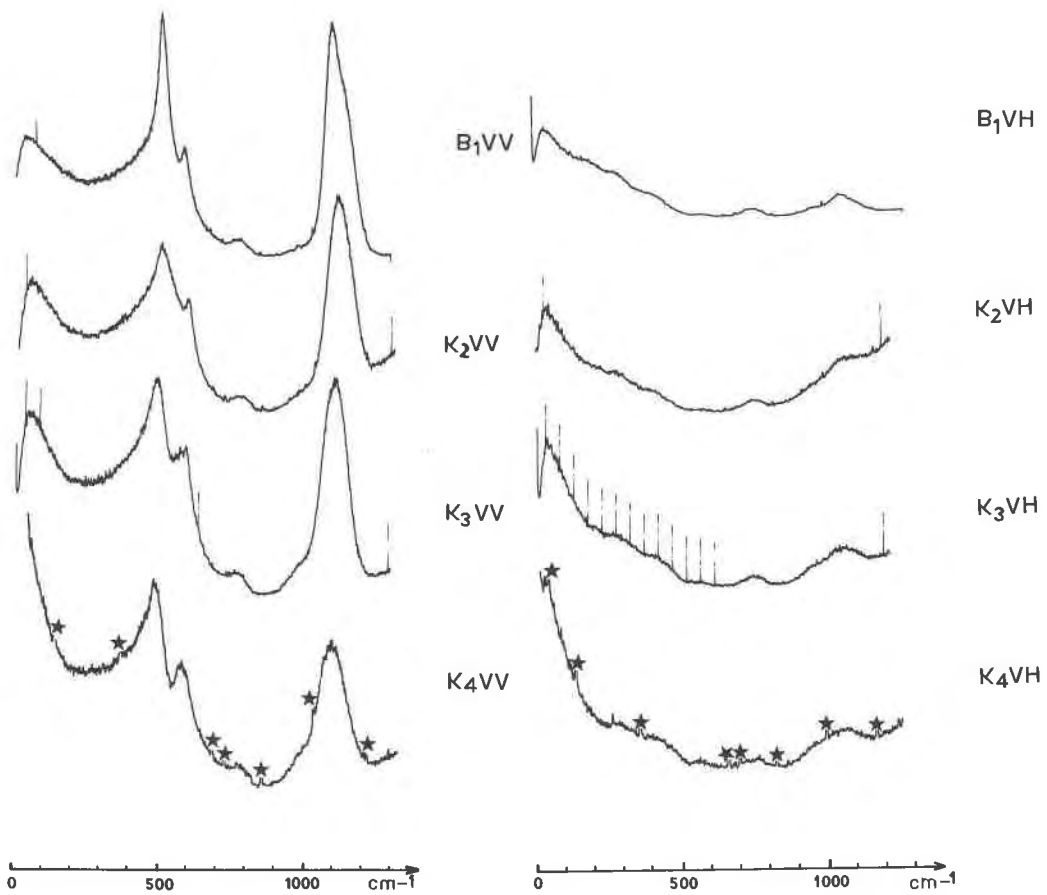

Fig. 3. Raman diffusion spectra of K series samples.

Physics 165Ar+ laser, scattered at 90° into a Coderg pHo double monochromator. The signal was detected by a Hamamatsu R829 photomultiplier and displayed after amplification on a chart recorder. VV (parallel polarization) and VH (perpendicular polarization) spectra were recorded and are displayed on Figures 2 and 3.

In order to improve the signal/noise ratio, the high frequency part of the spectra was iterated from 3 to 30 times and summed digitally on a microcomputer. These iterated spectra are shown in Figures 4 and 5.

Experimental results

In addition to the "thermal population" band, common in the Raman spectra of silicate glasses (Piriou and Alain, 1979), several large bands are visible (Figs. 2 and 3). Various studies of Raman spectra of silicate glasses and crystals have identified the major contributors of these large bands (McMillan and Piriou, 1983; Mysen et al., 1982a). The highly polarized band around 500 cm^{-1} is due to the vibration of BO in the plane bisecting the Si–Si segment. The silicon contribution to this movement is not yet well known. The depolarized band around 800 cm^{-1} is due to the symmetric vibration of two silicons about a BO. The highly polarized high frequency band, around 1100 cm^{-1} is due to Si–O stretching. More attention has been paid to this last band as it seems that its study can yield a great deal of structural information. The following part of this work is devoted to the study of this spectral region.

Table 1. Composition of samples studied

	SiO_2	K_2O	Al_2O_3
B 1	80.2	19.79	0
B 2	79.11	15.4	5.47
B 3	80.57	11.29	8.13
B 4	81.48	8.33	10.18
K 2	77.4	19.49	3.09
K 3	73.66	19.55	6.78
K 4	71.37	17.85	10.76

Various workers have recognized that the high frequency signal is the result of several overlapping bands (Mysen et al., 1982b) and of other physical effects. In this study, effects related to the prolongation background of the exciting radiation and the thermal population band are ignored as they have little effect on the high frequency envelope (Piriou and Alain, 1979; Seifert et al., 1982). The decomposition of the high frequency envelope into its components is necessary to facilitate a detailed interpretation of the spectra. Several methods have been used to undertake this decomposition. One of these methods

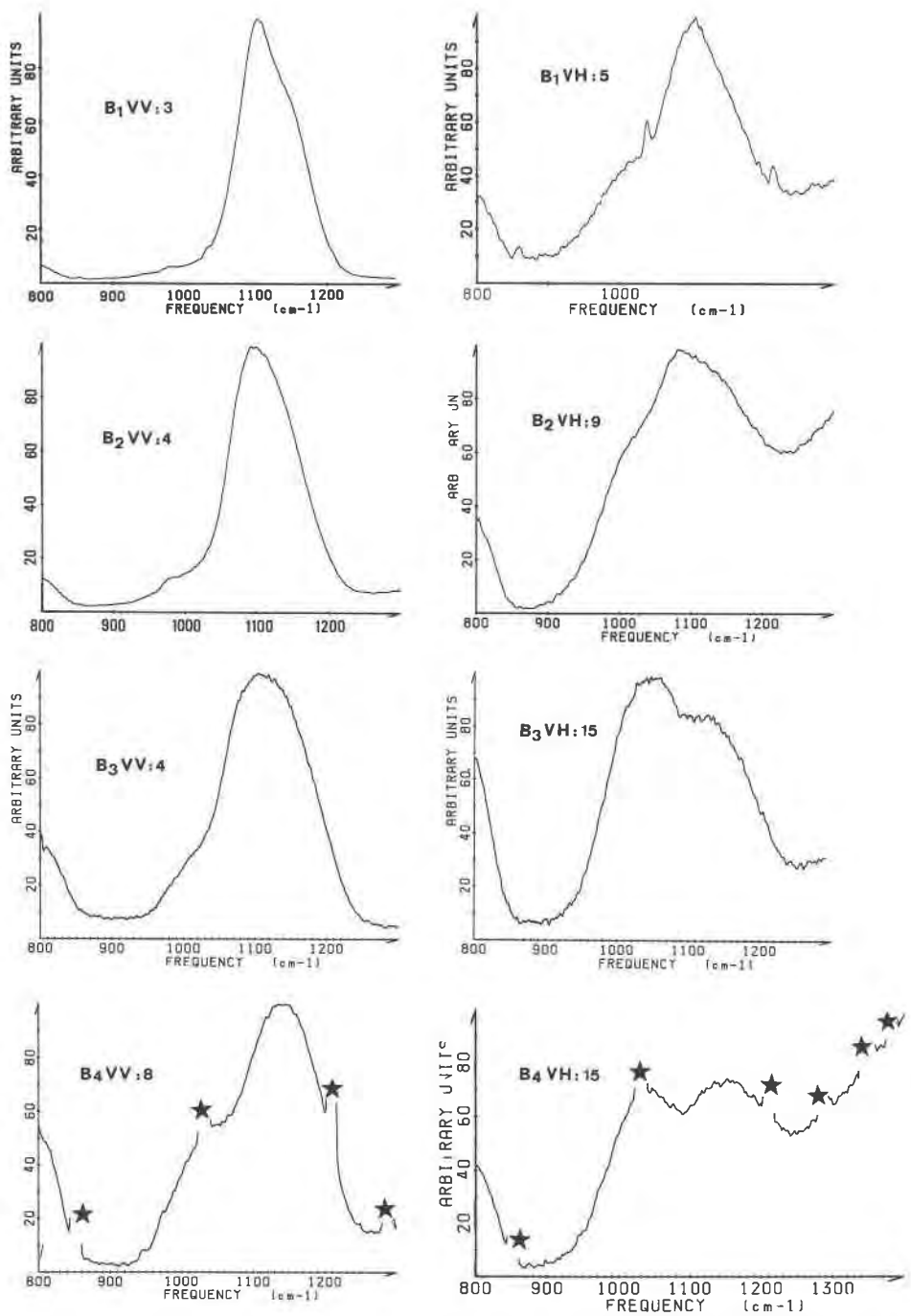

Fig. 4. Iterated high frequency VV and VH Raman spectra of B series samples. The number of iterations performed for each spectrum is shown next to the sample name.

is that presented by Mysen et al. (1982b). It is based on the minimization of a residual and is therefore of questionable value as it does not take into account the constraints arising from the evolution of the spectra with composition which should determine the evolution of the component bands. Moreover, the accuracy of such a method is greatly dependent on a good knowledge of poorly understood phenomena such as actual band shape, omitted bands and baseline corrections. A second method of decomposition involves constraining the positions and widths of component peaks, using the information acquired by considering the evolution of the spectra with composition (McMillan et al., 1982).

The method used in the present work attempts to take

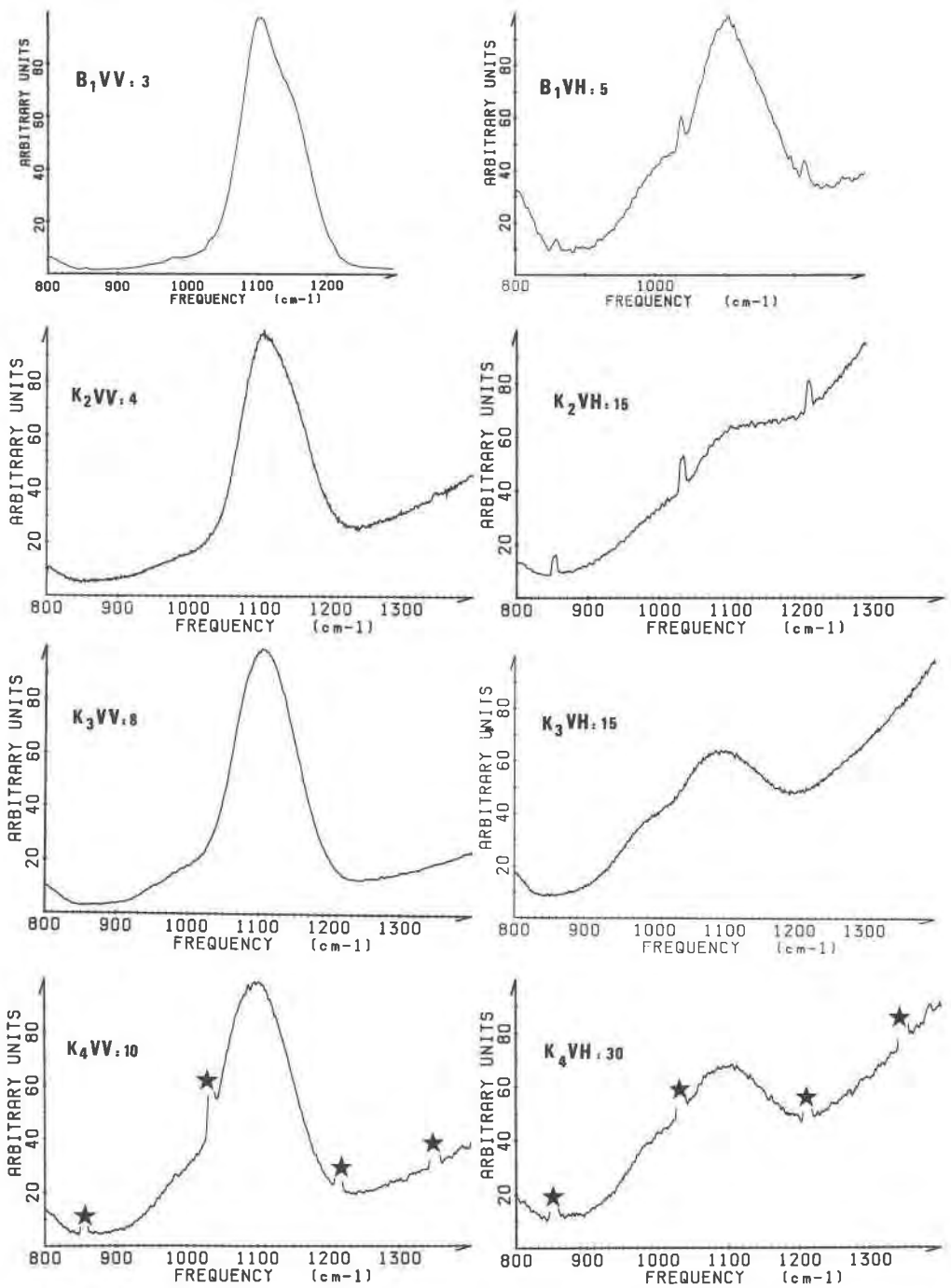

Fig. 5. Iterated high frequency VV and VH Raman spectra of K series.

into consideration the information deduced from the evolution of the spectra by limiting the variation of the band position and width within a given interval. Gaussian band shape is used (Seifert et al., 1982). The resulting theoretical spectrum is then calculated and can be compared visually with the experimental spectrum. A numerical value of the residual is also calculated, which enables minimization. The residual used here is of the type $R = \Sigma\,(\mathrm{CAL}-\mathrm{EXP})^2$ where CAL and EXP are respectively the calculated and experimental values. The effect of the minimization of R on the fitting parameters is actually minimal, since the variation of these parameters is very limited due to structural considerations. For this reason, no attempt was made to excessively minimize R, which was never smaller than the 3% point of the χ^2 distribution of the ideal residual (Law, 1973). The structural constraints for this model

Table 2. Proportion (%) of silicon environments (second neighbors) calculated with a random distribution

	B 1	B 2	B 3	B 4 Al_6*	B 4 Al_4*	K 2	K 3	K 4
Si_4	59.05	47.47	44.88	36.88	39.87	48.65	37.53	29.82
Si_3Al	0	26.26	36.23	36.67	39.85	15.54	27.63	35.97
Si_3K	33.24	12.61	3.57	5.13	1.36	22.86	14.04	6.16
Si_2Al_2	0	5.44	10.96	13.74	14.93	1.86	7.63	16.27
Si_2AlK	0	5.23	2.16	3.85	1.02	5.47	7.75	5.57
Si_2K_2	7.01	1.25	.10	.26	.01	4.01	1.96	.47
$SiAl_3$	0	.50	1.47	2.28	2.48	.09	.93	3.27
$SiAl_2K$	0	.72	.43	.96	.25	.43	1.42	1.68
$SiAlK_2$	0	.34	.04	.13	.008	.64	.72	.28
SiK_3	.65	.05	.001	.006	0	.31	.12	.01
Al_4	0	.01	.07	.14	.15	.001	.04	.24
Al_3K	0	.03	.02	.08	.02	.01	.08	.16
Al_2K_2	0	.02	.004	.01	.001	.02	.06	.04
AlK_3	0	.007	0	.001	0	.02	.02	.004
K_4	.02	0	0	0	0	.009	.002	0

* B 4 being an hyperaluminous composition, environment distribution have been calculated 2 different ways - supposing 3/4 of the excess aluminium remains a network former (B 4 Al_4) - supposing excess aluminium is a network modifier (column B 4 Al_6).

are based on the following hypothesis: (1) The Raman high frequency signal is characteristic of small size vibrational entities, silicon and its first and second neighbors (McMillan and Piriou, 1983; Piriou and McMillan, 1983a, b; McMillan, 1984) and (2) silicon second neighbors are randomly distributed.

Our approach will be to determine which component bands have to be considered and at what frequencies and to use this information to fit the high frequency envelope.

Determination of the component bands to be considered

In glasses of the compositions studied silicon first neighbors can be either BO's or NBO's. The second neighbor bonded to BO's can be Si or Al, while the second neighbor bonded to NBO's are K^+ ions. If we choose to represent each silicon environment by its four second neighbors, the 15 possible environments would be Si_4, Si_3Al, Si_3K, Si_2Al_2, Si_2AlK, Si_2K_2, $SiAl_3$, $SiAl_2K$, $SiAlK_2$, SiK_3, Al_4, Al_3K, Al_2K_2, AlK_3 and K_4. Here K is a network modifier, Si and Al are network formers. For simplicity, the charge balancing K^+ associated with each Al is not explicitly mentioned and K^+ mentioned are network modifiers. Using a simple random distribution, the proportions of each of these 15 environments can then be calculated for each composition: if p, q and (I − p − q) are the probabilities to have Si, Al or K as second neighbors, then the probability to have an aSibAl(4 − a − b)K environment is given by

$$p(Si_aAl_bK_{4-a-b}) = C_4^a C_{4-a}^b p^a q^b (1 - p - q)^{4-a-b} = \frac{4! p^a q^b (1 - p - q)^{4-a-b}}{a!b!(4 - a - b)!} \quad (1)$$

Since the coordination of Al in peraluminous melts is not entirely clear, the calculations for composition B4 were carried out in two different ways: (1) all excess aluminium assumed to behave as a network modifier and (2) assuming that ¼ of the excess aluminium is octahedrally coordinated, the remaining part being tetrahedrally coordinated. The results of all such calculations are reported in Table 2. We will see later on that Raman scattering provides some information concerning aluminium coordination.

Table 3. Silicon environments (second neighbors) and frequency of the Raman bands taken in consideration for the fitting of the high frequency part of the spectra

Silicon Environment	Si_4 (1)	Si_3Al (2)	Si_3K (3)	Si_2Al_2 (2)	Si_2AlK (4)	Si_2K_2 (3)	$SiAl_3$ (2)
Frequency (cm^{-1})	1070 1170 1210	1135	1100	1020	975	960	935

(1) Seifert et al (1982). (2) McMillan et al (1982). (3) Mysen et al (1980), Furukawa et al (1981), and Verweij and Konijnendijk (1976) (4) Determined in this study (see text).

By examining the data of Table 2, it is clear that only 7 silicon environments (Si_4, Si_3Al, Si_3K, Si_2Al_2, Si_2AlK, Si_2K_2, $SiAl_3$) are present in a large enough proportion to be possible to detect by Raman spectroscopy. All these seven environments except Si_2AlK exist in SiO_2–K_2O or SiO_2–$KAlO_2$ binary glasses and data concerning the frequencies of their Raman bands can be found in the literature and are given in Table 3. No data is available to allow us to determine the frequency of the Si_2AlK band, but it is well known that the vibration frequency is proportional to $\sqrt{k/m}$ where m is the reduced mass of the ions and k the force constant, which is related to the covalence of the bond. Thus, we expect the frequency of the band associated with Si_2AlK to be somewhere between those of Si_2Al_2 and Si_2K_2 (i.e., between 1020 and 960 cm^{-1}). It appears that all Si environments except Si_4 are characterized by only one high frequency band. It is very likely that this is just an approximation and that extra bands will be found in further studies. However they certainly are of very low intensity and the accuracy of the curve fittings does not enable us to determine them precisely.

Spectra fittings: comments

The spectra were fitted taking into account the environments reported in Table 3 with the frequencies of their bands. These frequencies sometimes differ slightly from what was expected from the literature, but we must remember that the cations present here are often different from those studied in the literature. VV and VH fits are shown in Figures 6 and 7, while the band frequencies, half widths and heights are reported in Table 4. Some comments concerning the decomposition are necessary.

The frequency similarity between VV and VH spectra is an argument for the consistency of the model. The slight frequency variations with composition can be attributed

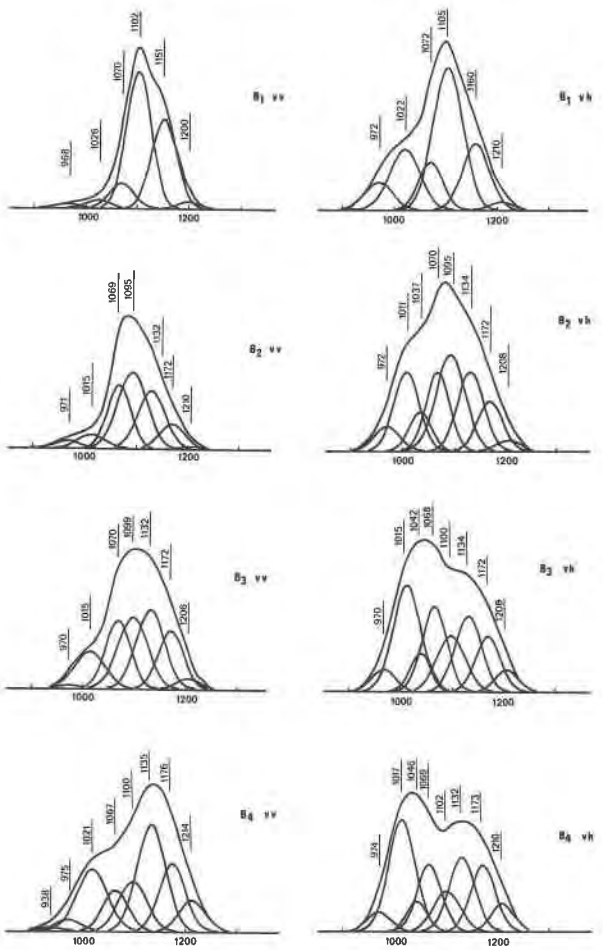

Fig. 6. Raman spectra fittings for B series samples. Frequency is in cm^{-1}.

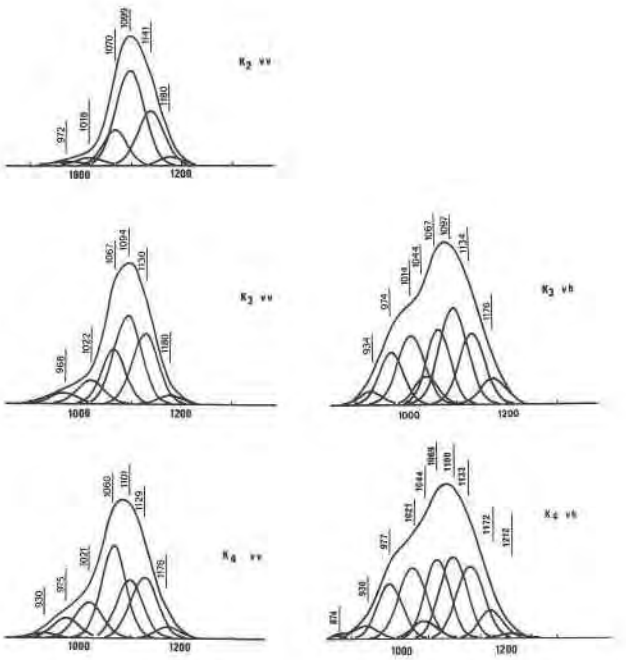

Fig. 7. Raman spectra fittings for K series samples. Due to the weak signal (see Fig. 5) K2VH spectrum could not be fitted.

to a weak influence from third neighbors. Due to their proximity, the bands that characterize Si_2K_2 and Si_2AlK could not be resolved. Their intensity is weak, and the accuracy of such a resolution would have been poor.

Two unexpected bands had to be used in the fittings. A highly depolarized band appears in the B1 spectra at 1026 cm^{-1} (VV) and 1022 cm^{-1} (VH) and shifts to higher wave numbers as alumina is added to the system (1037, 1042, 1046 cm^{-1} for B2, B3, B4). The fact that it appears mostly on VH spectra can be attributed to its strong depolarization. Considering that the frequency of this new band depends on composition, and to remain consistent with our model (constant frequency of a band), we suggest that this band is actually made up of 2 components 20 cm^{-1} apart. The low wave number components would characterize Si_4 or Si_3K while the higher component would characterize Si_3Al or Si_2Al_2. Addition of alumina to the system would then shift the band frequency to higher wave numbers. The 874 cm^{-1} band which appears in the K_4 VH spectrum can be attributed to the vibration of $SiAl_2K$ environment. This frequency is where it would be expected, between those of $SiAl_3$ and SiK_3, respectively at 935 and 850 cm^{-1} (see, for example, Furukawa et al., 1981 for the frequency of SiK_3).

Consideration of the intensity ratio of the 1100 (Si_3K) and 1135 cm^{-1} (Si_3Al) bands in the B series enables us to determine which of the two models suggested for Al coordination in B4 is better. This ratio decreases from B2 to B4, which is consistent with Al remaining tetrahedrally coordinated in B4. This result is obtained with just one slightly peraluminous (1.85 mole% excess Al_2O_3) composition and further studies are required before the coordination of non-charge-balanced aluminium can be clearly determined. However, this result shows that in composition B4, little or no aluminium is octahedrally coordinated. This confirms the results of McMillan and Piriou (1982) who concluded from a Raman spectroscopy study of the SiO_2–Al_2O_3 system, that for low alumina content, aluminium remains tetrahedrally coordinated.

These decompositions were obtained supposing a random distribution of silicon second neighbors. It is now possible to check the validity of this hypothesis.

Comparison of the experimental results with those expected from the random distribution

The decomposed spectra gave us qualitative results on the presence of various silicon environments in the glasses studied. But we can also extract some information concerning the relative proportions of these environments by comparing the areas of component bands. This will show if the distribution of silicon second neighbors is actually

Table 4. Raman band parameters used to fit the high frequency part of the spectra

Composition	VV Frequency (cm^{-1})	VV Half width (cm^{-1})	VV Amplitude*	VH Frequency (cm^{-1})	VH Half width (cm^{-1})	VH Amplitude*
B 1	968	56	1	972	61	5.4
	1026	57	1.75	1022	68	11.8
	1070	57	5	1072	54	9.2
	1102	55	27	1105	67	28
	1151	57	17.5	1160	62	13
	1200	50	1.4	1210	55	1.7
B 2	971	56	1.5	972	57	4.9
	1015	62	2.75	1011	57.7	15.65
				1037	49	7.8
	1069	52	12.5	1070	52	15.6
	1095	65	15	1095	65	19
	1132	61	11.45	1134	59	15.7
	1172	57	5	1172	57	10
	1210	55	.4	1208	54	2.25
B 3	970	45	.6	970	53	4.4
	1015	68	7.3	1015	61	21
				1042	49	7.5
	1070	55	13.4	1068	55	16.8
	1099	65	14	1100	63	11.1
	1132	62	15.5	1134	60	14.9
	1172	57	11.5	1172	56	11
	1206	52	2	1208	53	4.4
B 4	938	50	.75			
	975	57	1.55	972	52	4
	1021	69	8.2	1017	61	22
				1046	45	6
	1067	57	5.45	1069	55	13.2
	1100	64	6.58	1102	61	7.9
	1135	64	14.15	1132	58	14.6
	1176	59	9	1173	56	13
	1214	61	4.2	1210	52	5.5
K 2	972	75	.75			
	1018	65	1.5			
	1070	55	7			
	1099	65	19.7			
	1141	60	10.8			
	1180	58	1.8			
K 3				934	50	2.8
	968	60	2.15	974	56	10.5
	1022	61.5	4.7	1014	62	13.7
				1044	54	5.7
	1067	54	10.9	1067	55	14.85
	1094	63	17.5	1097	64	19.15
	1130	60	14	1134	59	14.1
	1180	58	1.8	1176	57	5.23
K 4				874	27	.75
	930	55	.7	930	55	2.65
	975	60	2.7	977	57	10.9
	1021	63	4.8	1021	63	13.9
				1044	55	3.62
	1069	57	12.3	1069	56	15.6
	1101	60	7.75	1100	60	16.1
	1129	62	8.1	1133	62	14.2
	1176	55	1.58	1172	53	5.7
				1212	43	1.15

* Peak heights are only relative and have no absolute meaning. They cannot be compared from one spectrum to another.

of the random type and if not, what kinds of attractive or repulsive interactions are present between these cations.

It would be desirable to calculate, from the Raman band intensities, the proportion of the different silicon environments present in the glasses. This is theoretically possible and has been successfully performed by Seifert et al. (1981b) for the binary system SiO_2–CaO. A set of linear equations of the form:

$$S_i = P_i a_i \tag{2}$$

where P_i describes the proportion of i species in the glass, S_i is the area of the Raman band corresponding to species i, and a_i the normalized cross section, was solved. The very few species present in a binary system makes this a satisfactory method. However, in a ternary system, solving such a set of equations would require one to study a number of compositions that is beyond the scope of this paper. Instead we shall consider the ratios of band intensities. Using ratios effectively cancels out unknowns and allows acquisition of qualitative information on the relative proportions of silicon environments. Moreover, a comparison of the results given by VV and VH spectra can be used as a test of the reliability of the fits.

Consistency of the fittings

In the following calculations carried out on the fittings we assume that the cross sections (a_i) do not vary with composition. This is very likely considering the small compositional variations. However, in our case, no reproducible geometric conditions were used to run the spectra. Instead of cross sections, we then prefer to talk about an "experimental efficiency" for each composition, defined as

$$S_i^\alpha = a_i^\alpha p_i^\alpha$$

S_i^α and p_i^α have the same meaning as S_i^α and p_i^α in (2), with α referring to composition. a_i^α is the experimental efficiency of i in composition α. a_i^α is then composition dependent. However, relation (3) is always true:

$$\frac{a_i^\alpha}{a_j^\alpha} = \frac{a_i^\beta}{a_j^\beta} \tag{3}$$

and comparing VV and VH spectra, we can write:

$$\frac{\left(\frac{S_i^\alpha}{S_j^\alpha}\right)_{VV}}{\left(\frac{S_i^\beta}{S_j^\beta}\right)_{VV}} = \frac{\left(\frac{S_i^\alpha}{S_j^\alpha}\right)_{VH}}{\left(\frac{S_i^\beta}{S_j^\beta}\right)_{VH}} \tag{4}$$

Relation (4) is used to test the consistency of the fitting, no matter which model we choose as a working basis, since we do not take the "P's" into consideration.

The accuracy we expect on the band area is fairly poor as two solutions having the same residual can display band areas differing by as much as 20% (i.e., solutions are non-unique). Both members of relation (4) have been calculated for spectra B2, B3, B4, K3, K4 and for bands at 1020, 1070, 1100 and 1135 cm^{-1}. K2 VH could not be fitted due to the weak signal. The four bands were chosen for their fairly strong intensity which minimizes the errors. In Table 5, we report the VV and VH values from relation (4) and we can see that the agreement is quite good, especially for column Si_3Al/Si_3K. To evaluate the quality of the fitting model, we can define a level of confidence C which is the extreme value of the VV/VH ratio tolerated. We can then plot as a function of C the number of (VV, VH) pairs that lies within the level of confidence that is (VV, VH) pairs such as $1/C < VV/VH < C$. The curve is shown in Figure 8 for values of C between 1 and 2.1. We can see that for C = 1.5, we have 26 out of 50 pairs that lie within the level of confidence. This number grows

Table 5. $\left(\frac{S_i^\alpha}{S_j^\alpha} \times \frac{S_j^\beta}{S_i^\beta}\right)$ terms for VV and VH values, where S_i^α is the area of the band characterizing environment i in composition α

		Si_4/Si_3Al*	Si_4/Si_3K*	Si_3K/Si_2Al_2	Si_3Al/Si_3K	Si_3Al/Si_2Al_2
B2/B3	VV**	1.237	.846	2.979	.683	2.037
	VH**	.864	.519	2.398	.6	1.441
B2/B4	VV	2.718	.934	7.227	.343	2.485
	VH	1.059	.462	3.588	.436	1.567
B2/K3	VV	1.364	1.292	1.482	.947	1.403
	VH	1.194	1.021	.841	.855	.719
B2/K4	VV	.692	.481	3.545	.695	2.467
	VH	.893	.784	1.139	.878	1
B3/B4	VV	2.196	1.104	2.425	.502	1.219
	VH	1.226	.891	1.495	.726	1.087
B3/K3	VV	1.102	1.526	.497	1.384	.689
	VH	1.382	1.967	.35	1.423	.499
B3/K4	VV	.559	.569	1.189	1.017	1.211
	VH	1.033	1.51	.475	1.461	.694
B4/K3	VV	.501	1.382	.205	2.754	.564
	VH	1.127	2.207	.234	1.958	.458
B4/K4	VV	.254	.515	.49	2.024	.992
	VH	.843	1.695	.317	2.01	.638
K3/K4	VV	.507	.372	2.391	.734	1.757
	VH	.748	.767	1.355	1.026	1.391

* For Si_4, the band at 1070 cm^{-1} was choosen.

** Similarity of VV and VH terms show the consistency of the fittings. The agreement is best for (Si_3Al/Si_3K) column.

to 42 out of 50 for C = 2.1. Considering the poor accuracy expected from the fitting, it appears that the overall consistency of the fitting is quite satisfactory. Indeed, the derivative of the (smoothed) curve of Figure 8 is gaussian shaped, with a maximum around 1.45. We then have an average error of 45%. The normal distribution of the error shows that we have a consistent model, although with a large error margin. For the most intense bands (Si_3Al, Si_3K), this error is reduced to 20%.

With the consistency of the fittings checked, we can now compare equilibria between various species, these equilibria being calculated (1) with the random distribution model and (2) with the spectroscopic data.

Comparison of experimental and random equilibria

Given the seven species and three cations considered in this treatment, four linearly independent relationships exist among the species:

$$Si_4 + Si_2Al_2 \leftrightarrow 2\ Si_3Al \quad (I)$$

$$2\ Si_3K \leftrightarrow Si_4 + Si_2K_2 \quad (II)$$

$$Si_3K + Si_2AlK \leftrightarrow Si_2K_2 + Si_3Al \quad (III)$$

$$Si_3K + SiAl_2K \leftrightarrow Si_2K_2 + Si_2Al_2 \quad (IV)$$

These four equilibria are not unique, as any linearly independent set will suffice. However, we have chosen these particular relationships for the following reasons:

Consideration of equilibrium (I) will inform us on the mutual interactions between Al ions, in the absence of NBO's. Equilibrium (II) will inform us of the mutual interactions between NBO's, while equilibria (III) and (IV) will inform us of the interactions between Al and NBO's.

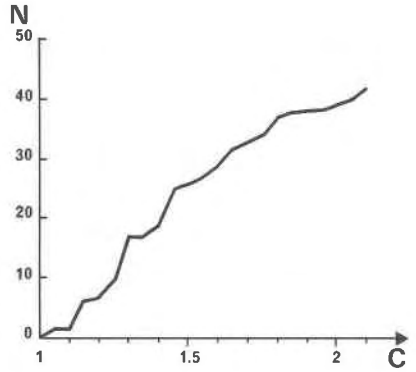

Fig. 8. Plot of number of points N lying within the level of confidence C vs. C, i.e. number of ratios such that

$$\frac{1}{C} < \frac{\left(\frac{S_i^\alpha}{S_i^\beta} \times \frac{S_j^\beta}{S_j^\alpha}\right)_{VV}}{\left(\frac{S_i^\alpha}{S_i^\beta} \times \frac{S_j^\beta}{S_j^\alpha}\right)_{VH}} < C$$

where S_i^α is the area of band of frequency i for composition α. This plot shows the consistency of the spectral fittings (see text).

To evaluate the displacement of the four equilibria we can write a relationship similar to equation (4):

$$\left(\frac{p_i^\alpha}{p_i^\beta} \times \frac{p_j^\beta}{p_j^\alpha}\right) = \left(\frac{S_j^\beta}{S_j^\alpha} \times \frac{S_i^\alpha}{S_i^\beta}\right) \quad (5)$$

The left term is calculated assuming a random distribution and reported in Table 6 ("RAN" line). The right term is calculated from the experimental data and reported on VV and VH lines.

To investigate the displacement of equilibrium (I) we can evaluate these terms for the bands associated with Si_3Al and Si_2Al_2 and with Si_4 and Si_3Al, i.e.,

(i, j) = (Si_3Al, Si_2Al_2) (1135 and 1020 cm^{-1})
(i, j) = (Si_4, Si_3Al) (1070, 1135)

From Table 6, we see that calculated and experimental terms are equal within the margin of error expected from Figure 8 (45%). Moreover, the differences between experimental and calculated values seem randomly distributed around zero.

For equilibria (II, III and IV) we can consider terms such that, respectively

(i, j) = (Si_4, Si_3K) (1070, 1100)
(i, j) = (Si_3Al, Si_3K) (1135, 1100)
(i, j) = (Si_2Al_2, Si_3K) (1020, 1100)

and we realize that calculated and experimental terms are not equal at all, even within the 45% error margin and we have the following inequalities:

$$\left(\frac{S^{\alpha}_{1070}}{S^{\beta}_{1070}}\right)\left(\frac{S^{\beta}_{1100}}{S^{\alpha}_{1100}}\right) > \left(\frac{p^{\alpha}_{1070}}{p^{\beta}_{1070}}\right)\left(\frac{p^{\beta}_{1100}}{p^{\alpha}_{1100}}\right) \quad (6)$$

$$\left(\frac{S^{\alpha}_{1135}}{S^{\beta}_{1135}}\right)\left(\frac{S^{\beta}_{1100}}{S^{\alpha}_{1100}}\right) > \left(\frac{p^{\alpha}_{1135}}{p^{\beta}_{1135}}\right)\left(\frac{p^{\beta}_{1100}}{p^{\alpha}_{1100}}\right) \quad (7)$$

$$\left(\frac{S^{\alpha}_{1020}}{S^{\beta}_{1020}}\right)\left(\frac{S^{\beta}_{1100}}{S^{\alpha}_{1100}}\right) > \left(\frac{p^{\alpha}_{1020}}{p^{\beta}_{1020}}\right)\left(\frac{p^{\beta}_{1100}}{p^{\alpha}_{1100}}\right) \quad (8)$$

valid when α has a higher network modifier content than β (i.e., a higher $[K_2O$–$Al_2O_3]$ content).

Interpretation and discussion

Since experimental and calculated data coincide well for equilibrium (I) we conclude that aluminium is randomly distributed among totally polymerized silicon environments. This spectroscopic observation is consistent with and confirms the thermodynamic models and measurements of Flood and Knapp (1968) and Navrotsky et al. (1982) who concluded that in the silica rich part of the system SiO_2–$KAlO_2$, aluminium was randomly distributed in the network, here totally polymerized.

However, inequality 6 shows that equilibrium II is displaced to the right, meaning that NBO's are not randomly distributed. This is unexpected, as Raman spectroscopic studies of the systems SiO_2–K_2O and SiO_2–Na_2O by Furukawa et al. (1981) and Verweij and Konijnendijk (1976) show that the intensity of the band characteristic of silicon with one BO is maximum at the disilicate composition, which is consistent with a random distribution of NBO's in these binary systems.

Likewise, according to inequalities 7 and 8, it is clear that equilibria III and IV are also displaced to the right, and we observe the migration of Al towards the more polymerized silicon environments and the concentration of K in the less polymerized ones. This confirms the results of Hess and Wood (1982) who studied the distribution of various elements between two immiscible liquids and who found that, in the presence of alkali, Al tends to concentrate in the more polymerized phase. This suggests that in the compositions studied, there exist repulsive interactions between Al and NBO's. The existence of such constraints on the cationic repartition in glasses can be predicted from the papers of de Jong and Brown (1980a, b) who, through molecular orbital calculations, described various interactions in glasses. Among them, substitution of Si by Al will lead to an increased repulsive effect from BO's bonded to Al, due to an increase of the number of electrons on the non-bonded levels. Therefore, we can predict that neighboring NBOs, bonded to the same Si as Al, would be unstable due to a strong negative charge concentration. Moreover, the network modifying (and charge balancing) cation present here, K^+, has a very weak positive charge density and very little stabilizing effect on the NBO's.

Al–K repulsive interaction and the consequent stabilization of Al in more polymerized environments is then expected, and we can attempt to quantify this interaction,

Table 6. Comparison of experimental values (VV and VH) with values calculated with a random distribution (RAN), and with values calculated with a non-random distribution, for x = 0.55 and y = 4.65 (CAL)

		Si_4/Si_3Al	Si_4/Si_3K	Si_3Al/Si_3K	$Si_3AlSi_2Al_2$	Si_3K/Si_2Al_2
B2/B3	VV *	1.237	0.846	0.683	2.037	2.979
	VH *	0.864	0.519	0.6	1.441	2.398
	RAN **	1.459	0.3	0.205	1.460	7.096
	CAL **	1.459	0.593	0.406	1/353	3.226
B2/B4	VV	2.718	0.934	0.343	2.485	7.227
	VH	1.059	0.462	0.436	1.567	3.588
	RAN	1.806	0.527	0.291	1.807	6.195
	CAL	1.806	0.941	0.52	1.699	3.262
B2/K3	VV	1.364	1.292	0.947	1.403	1.482
	VH	1.194	1.021	0.855	0.719	0.841
	RAN	1.331	1.408	1.057	1.333	1.258
	CAL	1.331	1.011	0.76	1.2	1.7
B2/K4	VV	0.692	0.481	0.695	2.467	3.545
	VH	0.893	0.784	0.878	1	1.139
	RAN	2.18	0.777	0.356	2.183	6.115
	CAL	2.18	1.229	0.564	2.063	3.659
B3/B4	VV	2.196	1.104	0.502	1.219	2.425
	VH	1.226	0.891	0.726	1.087	1.495
	RAN	1.238	1.756	1.418	1.242	0.872
	CAL	1.238	1.585	1.28	1.255	0.98
B3/K3	VV	1.102	1.526	1.384	0.689	0.497
	VH	1.382	1.967	1.423	0.499	0.35
	RAN	0.912	4.691	5.143	0.499	0.177
	CAL	0.912	1.704	1.868	0.953	0.511
B3/K4	VV	0.559	0.569	1/017	1.211	1.189
	VH	1.033	1.51	1.461	0.694	0.475
	RAN	1.494	2.59	1.733	1.501	0.861
	CAL	1.494	2.071	1.386	1.525	1.099
B4/K3	VV	0.501	1.382	2.754	0.564	0.205
	VH	1.127	2.207	1.958	0.458	0.234
	RAN	0.736	2.671	3.626	0.74	0.203
	CAL	0.736	1.075	1.459	0.75	0.521
B4/K4	VV	0.254	0.515	2.024	0.992	0.49
	VH	0.843	1.695	2.01	0.638	0.317
	RAN	1.206	1.475	1.222	1.207	0.987
	CAL	1.206	1.306	1.082	1.211	1.121
K3/K4	VV	0.507	0.372	0.734	1.757	2.391
	VH	0.748	0.767	1.026	1.391	1.355
	RAN	1.638	0.552	0.337	1.6	4.859
	CAL	1.638	1.215	0.742	1.596	2.151

* VV and VH terms are explained in table 5.

** RAN and CAL are $\left(\frac{p^{\alpha}_i}{p^{\alpha}_j} \times \frac{p^{\beta}_j}{p^{\beta}_i}\right)$ where p^{α}_i is the proportion of environment i in composition α given in table 2 for RAN and table 8 for CAL. For B4, RAN terms from B4 Al4 column

by representing it as the coefficient x of a conditional probability:

$$p(Al\backslash K) = xp(Al)$$

where $p(Al\backslash K)$ indicates the probability of having an Al atom linked to a silicon atom if there is already a K atom linked to this silicon and p(Al) refers to the probability used before such as p(Si) = p, p(Al) = q, p(K) = 1 − p − q = r.

Another obvious (attractive) interaction is that between 2 K^+ ions which can be represented as y such that

$$p(K\backslash K) = yp(K).$$

As a result of x and y being different from 1, four other parameters have to be considered:

$$p(Si\backslash K) = zp(Si) \qquad p(Al\backslash Al) = Bp(Al).$$
$$p(Si\backslash Al) = Dp(Si) \qquad p(Si\backslash Si) = Ap(Si).$$

Table 7. Values of (x, y) for some values of C, level of confidence. The residual of the fitting R is indicated

C	x	y	R	R for x = y = 1
1.55	0.45	4.76	29.6602	201.657
1.60	0.5	4.66	33.029	205.535
1.65	0.6	4.64	38.3164	210.938
1.70	0.6	4.64	38.3164	210.938
1.75	0.6	4.64	39.591	212.11
1.80	0.52	4.66	42.0316	248.706
1.85	0.52	4.66	43.9834	250.654
1.90	0.52	4.66	43.9834	250.654
1.95	0.52	4.66	43.9834	250.654
2.00	0.52	4.66	44.2006	250.946

Since our concern is to evaluate x and y, we want to calculate the probabilities as a function of x and y only and then to fit x and y.

Determination of the new probabilities of the silicon environments

If we can distinguish the 4 second neighbors of silicon, we can for example calculate the probability of the (AlSiKAl) environment where the first second neighbor of silicon is Al, it second one is Si, etc.

We get:

$$p(\text{AlSiKAl}) = p(\text{Al}\backslash\text{SiKAl})p(\text{SiKAl})$$

where p(Al\SiKAl) is the probability of Al being the fourth second neighbor of silicon knowing that Si, K, Al are the first, second and third second neighbors of silicon. And since

$$p(\text{SiKAl}) = p(\text{Si}\backslash\text{KAl})p(\text{KAl})$$

and

$$p(\text{KAl}) = p(\text{K}\backslash\text{Al})p(\text{Al})$$

we finally have

$$p(\text{AlSiKAl}) = p(\text{Al}\backslash\text{SiKAl})p(\text{Si}\backslash\text{KA1})p(\text{K}\backslash\text{A1})p(\text{A1})$$

and since

$$p(\text{Al}\backslash\text{SiKAl}) = \text{DxBp(Al)}$$
$$p(\text{Si}\backslash\text{KAl}) = \text{ZDp(Si)}$$
$$p(\text{K}\backslash\text{Al}) = \text{xp(K)}$$

we get

$$p(\text{AlSiKAl}) = x^2D^2ZBpq^2r.$$

Taking AlSiKAl in a different order would have yielded the same result and thus

$$p(\text{SiAl}_2\text{K}) = C_4^3C_3^2pq^2rx^2D^2zb$$

where $C_4^3C_3^2$ is the number of combinations for the $SiAl_2K$ environment.

Therefore, the new probability of any silicon environment is the probability calculated previously with the random distribution model multiplied by a correcting factor, easily determined as shown above.

Let us now determine Z, A, B, D as a function of x and y. Since

Table 8. Proportion (%) of the various silicon environments (second neighbors) calculated for the non-random distribution model, for x = 0.55 and y = 4.65

	x = 0.55			y = 4.65	
	B 2	B 3	B 4	K 3	K 4
Si_4	49.844	44.775	36.653	34.6	29.957
Si_3Al	27.571	36.144	36.635	25.477	36.132
Si_3K	7.07	3.77	4.893	4.966	5.226
Si_2Al_2	6.452	11.446	14.566	7.706	17.451
Si_2AlK	1.968	1.232	2.048	2.034	2.744
Si_2K_2	2.628	.533	1.172	2.305	1.774
$SiAl_3$	.757	1.685	2.73	1.134	4
$SiAl_2K$	.205	.14	.303	.304	.513
$SiAlK_2$	.326	.62	.182	.467	.36
SiK_3	3.004	.106	.573	4.083	1.356
Al_4	.036	.096	.203	.068	.366
Al_3K	.008	.005	.015	.016	.033
Al_2K_2	.011	.001	.007	.025	.019
AlK_3	.115	0	.016	.3	.066
K_4	0	0	0	16.51	0
Total*	101.41	100.05	100.35	122.45	100.81

* Due to the approximation, the total of probabilities were not always equal to 100% (see text) and data shown here have been normalized to 100%.

$$p(\text{Si}\backslash\text{K}) + p(\text{Al}\backslash\text{K}) + p(\text{K}\backslash\text{K}) = 1$$

we have

$$zp + xq + yr = 1.$$

Similarly

$$xr + Dp + By = 1$$
$$Ap + Dq + Zr = 1.$$

The last equation needed is that which states that the sum of the 15 probabilities is 1. However this would require solving a 6th degree polynomial and for the sake of simplicity we chose instead to state that A = D. This seems to be a rather reasonable approximation, since it only means that Al and Si will be affected the same way by the presence of a neighboring Si.

The probabilities can then be calculated for any (x, y) pair and then compared to the experimental results, which enables us to find the most suitable (x, y) set. To examine the effects of the errors on the experimental data (x, y) values were determined for different levels of confidence i.e., for a given C value, those (VV, VH) data taken into consideration were such that $1/C < VV/VH < C$. The most suitable (x, y) set was such that the residual $R = \Sigma (VV + VH - 2CAL)^2$ was minimum. The results of those calculations are reported in Table 7. Little variation is observed with various choices of C and we conclude that experimental errors have little effect over the final result, which will be taken as

$$x = 0.55 \text{ and } y = 4.65$$

The comparison of the experimental and calculated values for (x, y) = (0.55, 4.65) is shown on Table 6 ("CAL"

lines). The probabilities of Si environments have been calculated for (x, y) = (0.55, 4.65) and are shown in Table 8. Due to the approximation A = D, the sum of the probabilities is not always equal to 1 and have been normalized to 100%. The original total is also indicated and is very close to 100% for B2, B3, B4 and K4. It is still acceptable for K3.

The new probabilities have not been calculated for B1, because the absence of alumina makes it meaningless, or for K2, which was not used to determine x and y.

Conclusion

The numerical fitting of the thermodynamic parameters (x, y) confirms the results stated previously from equilibrium considerations. There exists a Al–NBO repulsive interaction which results in a concentration of Al in more polymerized environments and an affinity between NBO's such that:

$$p(Al\backslash K) = 0.55\ p(Al) \text{ instead of } p(Al)$$
$$p(K\backslash K) = 4.65\ p(K) \text{ instead of } p(Al)$$

(x, y) values are expected to be very dependent on the modifying cation (here K^+) density of charge: the negative charge concentration created by the association of Al and NBO around the same Si cannot be stabilized by K^+ ions, due to its weak density of charge. However, we expect this association could be stabilized by highly charged cations (for example Mg^{2+}) and in this case, we would expect an attractive interaction between Al and the modifying cation. This would predict that in ternary peralkaline systems the following equilibria

$$Si_3M + Si_2AlM \leftrightharpoons Si_2M_2 + Si_3Al$$
$$Si_3M + SiAl_2M \leftrightharpoons Si_2M_2 + Si_2Al_2$$
$$Si_4 + Si_2Al_2 \leftrightharpoons 2\ Si_3Al$$
$$2\ Si_3M \leftrightharpoons Si_4 + Si_2M_2$$

where M is a network modifier should move further to the left as the charge density of M increases.

Acknowledgments

Helpful reviews by M. P. Dickenson and D. M. Lindsley are greatly appreciated.

References

Brawer, S. and White, W. B. (1975) Raman spectroscopic investigation of the structure of silicate glasses. I, The binary alkali silicates. Journal of Chemical Physics, 63, 2421–2432.

De Jong, B. H. S. W. and Brown, G. E., Jr. (1980a) Polymerization of silicate and aluminate tetrahedra in glasses, melts, and aqueous solutions I: electronic structure of $H_6Si_2O_7$, $H_6AlSiO_7^-$, $H_6Al_2O_7^{--}$. Geochimica et Cosmochimica Acta, 44, 491–511.

De Jong, B. H. S. W. and Brown, G. E., Jr. (1980b) Polymerization of silicate and aluminate tetrahedra in glasses, melts, and aqueous soutions II: the network modifying effect of Mg^{2+}, K^+, Na^+, Li^+, H^+, OH^-, F^-, Cl^-, H_2O, CO_2, H_3O^+ on silicate polymers. Geochimica et Cosmochimica Acta, 44, 1627–1642.

Domine, F. and Piriou, B. (1983) Study of sodium silicate melt and glass by infrared reflectance spectroscopy. Journal of Non-Crystalline Solids, 55, 125–130.

Flood, H. and Knapp, W. J. (1968) Structural characteristics of liquid mixtures of feldspar and silica. Journal of the American Ceramic Society, 51, 259–263.

Furukawa, T., Fox, K. E., and White, W. B. (1981) Raman spectroscopic investigation of the structure of silicate glasses. III: Raman intensities and structural units in sodium silicate glasses. Journal of Chemical Physics, 75, 3226–3237.

Hess, P. C. and Wood, M. I. (1982) Aluminium coordination in metaluminous and peralkaline silicate melts. Contribution to Mineralogy and Petrology, 81, 103–112.

Konijnendijk, W. L. (1975) The structure of borosilicate glasses. Philips Research Report Supplement n° 1.

Konijnendijk, W. L. and Stevels, J. M. (1976) Raman scattering measurements of silicate glasses and compounds. Journal of Non-Crystalline Solids, 21, 447–453.

Law, A. D. (1973) Critical evaluation of "Statistical best fits" to Mössbauer spectra. American Mineralogist, 58, 128–131.

McMillan, P. (1984) Structural studies of silicates glasses and melts. Applications and limitations of Raman spectroscopy. American Mineralogist, 69, 622–644.

McMillan, P. and Piriou, B. (1982) The structural and vibrational spectra of crystals and glasses in the silica-alumina system. Journal of Non-Crystalline Solids, 53, 279–298.

McMillan, P. and Piriou, B. (1983) Raman spectroscopic studies of silicate and related glass structure—a review. Bulletin de Minéralogie, 106, 57–75.

McMillan, P., Piriou, B., and Navrotsky, A. (1982) A Raman spectroscopic study of glasses along the joins SiO_2–$CaAl_2O_4$, SiO_2–$NaAlO_2$ and SiO_2–$KAlO_2$. Geochimica et Cosmochimica Acta, 46, 2021–2037.

Mysen, B. O., Virgo, D., and Scarfe, C. M. (1980) Relations between the anionic structures and viscosities of silicate melts. A Raman spectroscopic study. American Mineralogist, 65, 690–710.

Mysen, B. O., Virgo, D., and Kushiro, I. (1981) The structural role of aluminum in silicate melts. A Raman spectroscopic study at one atmosphere. American Mineralogist, 66, 678–701.

Mysen, B. O., Virgo, D., and Seifert, F. A. (1982a) The structures of silicate melts. Implications for chemical and physical properties of natural magmas. Review of Geophysics and Space Physics, 20, 353–383.

Mysen, B. O., Finger, L. W., Virgo, D., and Seifert, F. A. (1982b) Curve fitting of Raman spectra of silicate glasses. American Mineralogist, 67, 686–695.

Navrotsky, A., Peraudeau, G., McMillan, P., and Coutures, J. P. (1982) A thermochemical study of glasses and crystals along the joins silica–calcium aluminate and silica–sodium aluminate. Geochimica et Cosmochimica Acta, 46, 2039–2047.

Piriou, B. and Alain, P. (1979) Density of state and structural forms related physical properties of amorphous solids. High Temperature High Pressure, 11, 407–414.

Piriou, B. and McMillan, P. (1983a) Ordre et spectroscopie vibrationnelle de silicates. Bulletin de Minéralogie, 106, 23–32.

Piriou, B. and McMillan, P. (1983b) The high-frequency vibrational spectra of vitreous and crystalline orthosilicates. American Mineralogist, 68, 426–443.

Roy, R. (1956) Aids in hydrothermal experimentation. II: Methods of making mixtures for both "dry" and "wet" phase equilibrium studies. Journal of the American Ceramic Society, 39, 145–146.

Seifert, F. A., Mysen, B. O., and Virgo, D. (1981a) Structural similarity between melt and glass relevant to petrological processes. Geochimica et Cosmochimica Acta, 45, 1879–1884.

Seifert, F. A., Mysen, B. O., and Virgo, D. (1981b) Quantitative determination proportions of anionic units in silicate melts. Carnegie Institution of Washington Yearbook, 80, 301–303.

Seifert, F. A., Mysen, B. O., and Virgo, D. (1982) Three dimensional network structure of quenched melts (glass) in the systems SiO_2–$NaAlO_2$, SiO_2–$CaAl_2O_4$ and SiO_2–$MgAl_2O_4$. American Mineralogist, 67, 696–717.

Sweet, J. R. and White, W. B. (1969) Study of sodium silicate glasses and liquids by reflectance spectroscopy. Physics and Chemistry of Glasses, 10, 246–251.

Verweij, H. and Konijnendijk, W. L. (1976) Structural units in K_2O–PbO–SiO_2 glasses by Raman spectroscopy. Journal of the American Ceramic Society, 59, 517–521.

Virgo, D., Mysen, B. O., and Kushiro, I. (1980) Anionic constitution of one atmosphere silicate melts. Implication for the structure of igneous melts. Science, 208, 1371–1373.

Manuscript received, March 6, 1984;
accepted for publication, September 3, 1985.